DEFLECTION HARDENING OF SUSTAINABLE FIBER-CEMENT COMPOSITES

P. R. L.Lima PhD*, Full Professor in the Department of Technology, Universidade Estadual de Feira de Santana, Av. Transnordestina, s/n, Novo Horizonte, CEP: 44036-900, Feira de Santana, Bahia, Brazil. +55 75 3161 8310

D. O. J. Santos, M.Sc., Post-graduate Program of Civil and Environmental Engineering, Universidade Estadual de Feira de Santana, Brazil

C. M. A. Fontes PhD, Adjunct Professor in Department of Technology, Universidade Estadual de Feira de Santana,, Brazil

J. A. O. Barros PhD, Full Professor in ISISE, Dept. Civil Engineering, Universidade do Minho, Campus de Azurém, Guimarães, Portugal.

R. D. Toledo Filho PhD, Titular Professor in Civil Engineering Department, COPPE, Universidade Federal do Rio de Janeiro, Rio de Janeiro, Brazil

*corresponding author: lima.prl@pq.cnpq.br

ABSTRACT

In the present study sisal fiber–cement composites reinforced with 4% and 6% of short fibers were developed and their physical–mechanical behavior was characterized. To ensure the composite sustainability and durability, the ordinary Portland cement matrix was modified by adding fly ash and metakaolin, and the natural aggregate was substituted by 10% and 20% of recycled concrete aggregate. Flat sheets were cast in a self-compacted cement matrix and bending tests were performed to determine the first crack, postpeak strength and toughness of the composites. Cyclic flexural tests were carried out to determine the stiffness variation of composite due to cracking formation and propagation. It can be seen that the reinforcement provided by short sisal fibers for recycled cement matrices guaranteed a composite with multiple cracking and an increase of strength after the first crack. Reduction of stiffness and increase the damping capacity of composite are verified with progressive cracking.

Keywords: Natural materials, Composite materials, Structural properties

List of notation (examples below)

ARF is the aspecto ratio of fiber = Vf.Lf/df

P is the applied load

L is the specimen's span length (= 300 mm)

b is the width of the plate's cross section

e is the thickness of the plate's cross section

ftd is the average indirect tensile strength

fc is the average compressive strength

E	is the elastic stiffness
Vf	is the fiber content, in volume
Lf	is the fiber length
df	is the fiber diameter

1. Introduction

Cement based materials are the most important building materials used in the world, as paste, mortar or concrete. However, their production is associated with major environmental problems due to large energy consumption, solid waste generation and consumption of natural resources. One solution to minimize this negative impact is to use nonconventional materials, called green materials and characterized by the use of local, renewable or recycled materials, which consume little energy for production and transport. Unfortunately, the image of these materials is associated with lower performance and few commercial applications are currently available in the world, which requires a search for green materials with high strength and durability.

The fiber cement industry is one of the most relevant in the construction sector, with large-scale use of cement and fibers. With the banning of asbestos fiber, the reinforcement of cement composite was replaced by polymeric fibers manufactured from fossil fuel, such as polypropylene fibers (PP) and polyvinylalcohol (PVA). However, the use of vegetable fibers as reinforcement of cement based matrix has demonstrated great potential: roofing tiles[1], large span tiles[2] and formwork slabs[3] have been produced further demonstrating the possibility of producing semi-structural constructive elements reinforced with high-performance cementitious composites[4,5]

The constructive elements reinforced with sisal fibers has the advantage of using biodegradable fibers, derived from renewable sources and low power consumption for production, which characterizes it as a sustainable building material[6]. However, due to the low fiber-matrix adherence, the high-performance composites were produced with long fibers and with the use of pressure molding or mineral microfibers resulting in higher production costs and limiting the type of building element. The use of short sisal fiber in conventional cement matrices doesn´t result in multiple cracking behavior, due to the difficulty in dispersing higher fiber volume fractions and fiber lengths higher than 25 mm. In order to produce a composite reinforced with short vegetable fibers that present deflection hardening (after crack initiation the flexural resistance increases with the deflection), a modification of the cement matrix and treatment of the fiber was developed in the present study.

The development of an appropriate matrix is achieved using chemical additives, mineral admixtures and appropriate fine aggregates with a particle size modified to ensure a good dispersion of the fibers in the matrix and the required fluidity for the mixture[7,8]. The use of mineral admixtures such as fly ash and metakaolin ensures an increase in mechanical strength and workability of the mixture, as well as the durability of fibers in an alkaline medium[9], and reduces the cement consumption making it more sustainable. Previous works[5,10] have shown that continuous sisal fiber cement-based composites produced with a matrix with low contents of calcium hydroxide preserved its original toughness and

strength even when subjected to 25 wetting and drying cycles, while ordinary cement based composites loses toughness and flexural strength after 10 cycles.

The refinement of the matrix can be obtained using fillers or aggregates obtained by recycling construction and demolition waste. Fine recycled aggregate has been used to produce mortar without a reduction of physical and mechanical properties when compared with conventional mortar[11,12]. In fibrocement, the fine particles (less than 75 μm) present in this recycled aggregate can contribute to the workability of fresh mixture and to the refinement of the pore structure of hardened matrix. Although studies indicate that the addition of fine recycled aggregate in relatively large percentages contributes to an increase in shrinkage and water absorption, leading to a reduction of the mechanical strength of the corresponding composite material[13,14], the use of lower levels, up to 20%, is recommended by standards[15].

The most serious concern with natural fibers is their hydrophilic nature, due to the presence of pendant hydroxyl and polar groups in various constituents, which can lead to poor adhesion between fibres and matrix[16]. Sisal fibers present a great capacity for water absorption[17], thus the swelling and shrinking of the fibers due to wetting and drying of composites in use may lead to cracking in the fiber-matrix interface. As a result, the mechanical properties of the composite reinforced with vegetable fibers are very sensitive to moisture content, to a greater extent than other fiber reinforced composites, in which the fibers are not hygroscopic. However, a reduction in the hydrophilicity of the fiber can be obtained through the use of wetting-drying cycles[18], with a reduction in the dimensional change of the fiber and an increase on the fiber-matrix adherence, allowing for a better flexural performance of the composite material[19].

The objective of this work is to develop sustainable cement based composites with natural fiber reinforcement and recycled matrix that can be used in semi-structural building elements. To obtain the new matrix, the fine natural aggregate was replaced by 10% and 20% of recycled concrete aggregate. Water absorption test and mechanical tests were carried out to investigate the effect of this aggregate replacement content on the properties of the matrix. The composites were reinforced with 4% and 6% of treated sisal fibers of 40 mm length, based on previous studies conducted by Ferreira[20], which evaluated composites with reinforcement content ranging from 2% to 6%, and fiber length of 25 to 50 mm. For the mechanical characterization of composites, compression, indirect tension and flexural tests (in monotonic and cyclic loading conditions) were executed.

2. Experimental Program
2.1 Materials
2.1.1 Sisal fiber
The sisal fibers (*Agave sisalana*) were collected in the city of Valente, state of Bahia – Brazil. They were extracted from the sisal plant leaves by semi-automatic decorticators in the form of long fiber bundles. In laboratory, the long fibers were first washed in hot water (50 °C), to remove surface residues from the extraction process, and then cut into short fibers of 40 mm length.

The fibers were subjected to a treatment with wetting-drying cycles to reduce water absorption and therefore its dimensional variation. Fiber treatment, conducted according to the method described by Ferreira[19], consisted in immersing the fibers in water (T ~ 23 °C) and their removal after saturation (3 h) for drying in a furnace at a temperature of 80°C (16 hours). After 16 h of drying, the furnace was allowed to cool down during a 5h period to the temperature of 23 °C in order to avoid possible thermal shock to the fibers. This procedure was repeated 10 times.

2.1.2 Aggregates

Construction and demolition waste (CDW) from a building demolition site in Feira de Santana (Northeast of Brazil) was used to produce the recycled aggregate. The composition of CDW was 56% of mortar, 27% of ceramic tiles and bricks, and 17% of concrete. The concrete phase of waste was crushed separately using a jaw crusher and screened in a 2.36 mm sieve to produce the fine recycled concrete aggregate (RCA) used in this work. The natural aggregate used was fine sand (NA).

To determine the physical properties of the fine aggregates absorption and specific weight tests were carried out, as shown in Table 1. As expected, the recycled aggregates presented higher presence of materials finer than 150 μm, which is attributed to the methodology of obtaining aggregates from concrete recycling. It can be observed that crushed aggregates have a large portion of fine grains, even when originated from granitic rocks[21]. The values of fine content and water absorption indicated in Table 1 are also compatible with the nature of the recycled concrete aggregate, and are in accordance with the values observed by Corinaldesi and Moriconi[11].

Table 1

Characterization of aggregates

Characteristic	Natural aggregate	Recycled aggregates
	NA	RCA
Maximum diameter (mm)	1.20	2.36
Fineness	1.73	2.11
Materials finer than 150 μm (%)	0.95	14.36
Absorption (%)	0.03	6.11
Unit weight (kg/dm³)	2.65	2.60
F-circle (see Fig. 2)	0.74	0.65

Fig. 1 shows the gradation curve of aggregates; manual granulometry was performed to determine the maximum diameter, the fineness and the amount of material finer than 150 µm; laser granulometry was used for the characterization of the material finer than 150 µm. Within the fine fraction (< 150 mm), Fig. 1b, the recycled aggregates appear to be more fine than the natural one.

The circular shape factor (F-circle in Fig. 2) of sand particles, shown in Table 1, was determined through SEM analysis as described in a previous work[22]. The samples were segregated by a sieve series and the fractions retained in 250 µm were cold mounted with epoxy resin, and subsequently

ground and polished in a conventional metallographic approach (see Fig. 2). The analysis of shape, summarized in Table 1, demonstrated that the natural sand sample presented a more rounded particle shape (F-circle ~ 0.74), as previously described[21], and confirmed the higher roundness of the natural aggregate when compared with the recycled one. The qualitative evaluation of the surface of particles by stereoscopic microscopy revealed that the surface texture of recycled aggregates is irregular and rougher.

X-ray diffraction (XRD) analysis, performed in a powder X-ray diffractometer (Bruker D8 Focus with Cu ka tube, 30 kV and 35 mA) was used to characterize the crystallographic structure of aggregates. The typical results presented in Fig. 3 reveal that the main components of the natural aggregate is SiO_2 (quartz), while the main components of RCA are $CaCO_3$ (calcite) and SiO_2 (quartz). This illustrates that RCA is mainly composed of sand and hydrated cement, similar to that observed by Chen[14]. All aggregates showed a crystalline structure.

2.1.3. Cementitious materials

The binder is composed of 33% of Portland cement CP II-F (Portland cement with filler), 27% of metakaolin (MK) and 40% of fly ash (FA), whose respective chemical compositions and specific gravity are presented in Table 2.

Table 2

Chemical composition and specific gravity of cement and pozzolanic materials

Chemical Component	CP II F-32	Metakaolin	Fly ash
CaO	73.09	-	1.94
SiO_2	13.64	46.22	51.58
SO_3	3.97	0.38	1.51
Al_2O_3	3.78	48.78	28.24
K_2O	0.39	0.64	3.39
SrO	0.30	-	-
TiO_2	0.30	1.41	1.30
MnO	0.06	-	1.51
ZnO	0.05	-	-
CuO	0.02	-	-
Fe_2O_3		2.30	
BaO		0.18	
Specific gravity (g/cm^3)	3.01	2.65	2.01

The percentage of fly ash and metakaolin aims to develop a matrix that is free of calcium hydroxide (CH) at 28 days of age, and to preserve the durability of the fibers as much as possible, as shown in previous research[5]. Thermal analyses were performed in cement paste and cement + MK/FA paste to determine the calcium hydroxide content. The tests were performed in a SDT Q600 from TA Instruments. Samples weighing 10 mg were submitted to a heating rate of 10°C/min until reaching

1000°C in a platinum crucible using 100 ml/min of nitrogen as the purge gas. The most important products of the hydration reactions are calcium silicate hydrate (C-S-H) and CH. With an increase of temperature in cement paste, it is possible to identify, using a derivative thermogravimetric (DTG) curve, the range of temperature correspondent to the dehydroxylation of the CH, and calculate the CH content of paste, using thermogravimetric (TG) analysis.

Fig. 4 shows thermogravimetric (TG) and derivative thermogravimetric (DTG) curves of the cement and cement+MK/FA after 28 days of curing. In the DTG curve of cement paste the peak between 380 C and 440 C corresponding the dehydration of calcium hydroxide, $Ca(OH)_2$ can be seen. For cement+MK/FA paste this peak does not exist due to the very small free lime content.

2.2. Composite production

The mixtures were divided into three groups: matrices; cement composites with 4% in volume (Vf) of fiber and cement composites with Vf=6%. In each group, three mixtures were produced and the difference between them is resumed to the content of recycled aggregate, as shown in Table 3. The aggregates substitution rate, in mass, was 10%RCA and 20%RCA. The water/binder ratio was kept constant and equal to 0.45.

Table 3

Mix proportions of natural (REF) and recycled aggregates matrices and composites (kg/m³)

Mix	Cement	Fly Ash	Metakaolin	Natural aggregate	Recycled aggregate	Water	SP	Fiber
Matrix								
REF.	314.52	381.24	257.34	476.55	-	428.90	24.71	-
10RA	314.41	381.11	257.25	428.75	47.64	428.75	24.71	-
20RA	314.31	380.98	257.16	380.98	95.24	428.60	30.86	-
Cement composite reinforced with 4% of fiber								
REF4F	301.74	365.75	246.88	457.18	-	411.47	59.26	36.57
10RA4F	301.64	365.63	246.80	411.33	45.70	411.33	68.13	36.56
20RA4F	301.54	365.51	246.72	365.51	91.38	411.19	74.02	36.55
Cement composite reinforced with 6% of fiber								
.REF6F	295.73	358.46	241.96	448.08	-	403.27	58.08	53.77
10RA6F	295.64	358.35	241.88	403.14	44.79	403.14	66.77	53.75
20RA6F	295.54	358.23	241.81	358.23	89.56	403.01	72.55	53.73

Since the water absorption rate of recycled aggregate is larger than natural aggregate (see Table 2), superplasticizer (SP) was added to the mixtures to avoid major modification of the water/cement ratio, and to maintain the consistency of matrix, measured by mini slump test, of about 140±10mm. A third generation superplasticizer (Glenium 51) with a solid content of 30.9% and specific gravity of 1.1 g/cm^3 was used to guarantee the good workability of the mixture. The viscosity modifier admixture

(VMA) Rheomac UW 410 with specific gravity of 0.7 g/cm^3, at a dosage of 0.05% relative to the binder, in weight, was also used, in order to avoid segregation during molding.

The mixtures were produced using a mixer with capacity of 20 dm^3. The following mixing procedure was used to produce the matrix. Cement and fly ash were homogenized in the mixer and then water and superplasticizer were added. Metakaolin and fine aggregate were added and mixed for 4 minutes at low speed (125 RPM). After this, the mixing process was stopped for 30 seconds to remove the material retained on the mixer walls. Then, the mixing procedure continued for 2 minutes at medium speed (220 RPM). The VMA was then added and mixed for another 2 minutes at 125 RPM. To produce the composites, the matrix was produced using the same procedures as described above. After 2 minutes mixing at medium speed, chopped sisal fibers of 40 mm length (Vf=4 % or 6%) were added, and mixed for 4 minutes at 125 RPM.

2.3. Test methods

The sisal fiber's microstructure was investigated using a scanning electron microscope (JEOL JSM-6460). The Fourier transform infrared (FTIR) spectroscopy method, using a Perkin Elmer spectrometer, was used to analyze the possible composition change of the sisal fiber after treatment. Tensile tests of fiber were performed in a TA.XT Plus Texture Analyzer with a load cell of 500 N. The tests were performed with 20 fibers using a displacement rate of 0.03 mm.s^{-1}. The fibers with a gage length of 50 mm were glued on a paper template for better alignment in the machine and for better gripping with the upper and lower jaws.

The apparent diameter of fiber was achieved using an optical microscope QUIMIS model Q711FT. The fiber strands were observed in the optical 10X lens (tenfold) and finally the mono-strand was photographed with a camera attached to the microscope. Then, the picture was transferred to the program MOTIC IMAGES PLUS 2.0 for the measurement of the fiber thickness. This thickness value is associated with the apparent diameter of the fiber, assuming a theoretical model in which the cross section is circular. However, it is known that the fiber section has multiple shapes and may vary along the length[23]. To reduce the error, sixty diameter measures were conducted for each treatment.

Water absorption test of matrix was carried out according to NBR 9778/09[24]. Three cylindrical specimens of 50 mm in diameter and 100 mm in height were used in each test.

Compressive tests were carried out in three cylindrical specimens of 100 mm in diameter and 200 mm in height, after 28 days of cure, according to NBR 5739[25] (equivalent to ASTM C39-04a). The specimens were tested on a 2000 kN Contenco testing machine at a rate of axial load of 1000 N/s. Indirect tensile tests, according to NBR 7222[26] (equivalent to ASTM C496), were carried out on three cylindrical specimens of 100 mm in diameter and 200 mm in height. The specimens were tested on a 2000 kN testing machine at a rate of axial loading of 500 N/s, and using a load cell of 50 kN. For the flexural test, initially, flat plates with dimensions of 400 mm x 400 mm x 10 mm were molded (see Fig.5a). The mortar mix was manually placed into a steel mould, followed by external vibration.

After 28 days of curing with immersion in water, the plates were cut in prismatic specimens with dimensions of 400 mm x 70 mm x 10 mm for the flexural tests. Bending tests were carried out with specimens of 28 days of age under displacement control at a crosshead rate of 0.3 mm/min in a Shimadzu UH-F 100 kN machine with load cell of 1 kN (Fig. 5b). Three specimens for each mix were tested under four-point bending configuration. Flexural stress was obtained using the following equation:

$$\sigma = \frac{PL}{be^2}$$

1.

The effect of the fiber on increment of toughness of the composite was measured using the Toughness Index (I_{20}) — defined by ASTM C1018-97 standard[27] as the ratio between the area under the curve from zero to 10.5 times the first-crack deflection and the triangular area under the curve up to first-crack deflection.

By using a digital camera possessing a 10X macro zoom lens and frame grabber capable of capturing images of 480 x 640 in resolution at 60 s intervals, the cracking patterns at regular time intervals were recorded. These images were used to measure the crack formation process during the flexural tests following the methodology proposed by Silva[28]. Photos of the tension face in the flexural tests were taken using a mirror positioned below the specimen, as shown in Fig. 5b.

3. Experimental results and discussion
3.1 Treatment of sisal fiber

A reduction in the fiber hydrophilicity can be achieved by rewetting and drying cycles to promote hornification, which is the stiffening of the polymeric structure present in lignocellulosic materials. When wood pulp or fibers are dried, the internal fiber volume shrinks, because of structural changes, which can cause a significant loss of large pores and a reduction of surface area of fibers. If fibers are resuspended in water, the original water-swollen state is not regained[29]. Fig. 6 shows the cross section of sisal fiber. After 10 cycles, the sisal fiber shows a reduction of volume of lumen and the presence of micro-cracks across fiber cells. The fiber equivalent diameter decreases with treatment (see Table 4) since there is a shrinkage of fiber due to hornification starting in the final phase of drying, when tightly bound water leaves the microstructure of the fibre, causing reversible shrinkage in the direction of the fibre width[18].

Fig. 7 shows the normalized FTIR spectrum of untreated and treated sisal fiber. An infrared spectrum represents a fingerprint of a sample with absorption peaks corresponding to the frequencies of vibrations between the bonds of the atoms making up the material. Because each different material is a unique combination of atoms, no two compounds produce the exact same infrared spectrum. Therefore, infrared spectroscopy can result in a positive identification of the chemical alteration of sisal fiber due to treatment. The peak at 1733 cm^{-1} is assigned to the hemicelluloses and the peak at 1240 cm^{-1} is assigned to lignin[30,31]. The peak at 3300 cm^{-1} and the peak at 1630 cm^{-1} are due to the

characteristics of axial vibration of the hydroxyl group of cellulose[32]. The disappearance of any of these peaks indicates a change in the chemical composition of the fiber due to treatment. The presence of all peaks in the spectrum of treated fiber can be noted however, which indicates that the treatment applied does not alter the chemical structure of the fiber sisal.

The Fig. 8 presents the typical results of tensile test in terms of stress-strain behavior. The experimental results presented in Table 4 indicate that the treatment with 10 cycles influenced fiber strength (reduction of about 3%) and elastic modulus (reduction of about 21%), associated to the formation of microcracking of sisal fiber (see Fig.6).

Table 4
Experimental results of direct tension tests of sisal fiber (mean values and coefficient of variation in percentage)

Cycles	Sisal fiber		
	Apparent diameter (μm)	Tensile strength (MPa)	Elastic Modulus (GPa)
0	280 (27)	363 (26)	20.06 (52.9)
10	244 (27)	353 (27)	15.72 (42.4)

3.2 Characterization of matrices

Table 5 shows the experimental results of matrices. Due to the higher water absorption of recycled aggregate (see Table 2), the water absorption of recycled mortar is higher (up to 11.7%) than reference mortar. The porosity of recycled aggregate (RA) also contributes to an increase in water absorption and porosity of recycled mortar[13].

Table 5: Physical properties of matrices (coefficient of variation in percentage)

Mix	Water absorption			Mechanical Properties	
	Absorption (%)	Porosity (%)	Density (g/cm^3)	fc (MPa)	ftd (MPa)
REF	19.28 (0.9)	29.52 (0.9)	2.17 (0.3)	30.42 (0.8)	2.13 (11.6)
10RA	21.08 (1.1)	32.60 (1.0)	2.30 (0.4)	30.24 (0.3)	2.09 (19.4)
20RA	21.53 (0.6)	32.17 (0.1)	2.20 (0.5)	31.27 (2.0)	2.06 (15.5)

While the addition of 10% of RA results in an increase in physical properties compared to reference matrix, it can be seen that the increment of content of RA to 20% reduces the porosity and density of mortar. This fact can be associated with the presence of finer material in RA that promotes a refinement of porosity. Thus, the negative effect of water absorption of RA[33] is compensated by the filler effect of smaller grains. In addition, the increase of the superplasticizer permits a better homogenization of the material (self compacting mix) and reduces the water sorptivity of mortar[34].

The experimental results corresponding to mechanical tests of matrices are included in Table 5. For the percentage of recycled aggregate adopted, the compressive strength was not affected, while a tendency for a small decrease (about 3.3%) in the indirect tensile strength was observed. This small

influence of the replacement of natural aggregates by recycled ones (up to 20%) can be caused by the relatively high content of cement (both hydrated and non-hydrated) present in the fine recycled concrete aggregate[35]. The splitting strength shows a decrease of about 4% with the increase of NA replacement with RA, also identified by Evangelista and Brito[12].

3.3 Evaluation of composites

In table 6 the mechanical results of cement based composites are presented. Fig. 9 shows the envelope and the average of the flexural stress versus the central deflection relationship of the 4 point bending tests. The graphics of this figure also include the relationship between the central deflection and the average crack spacing. The relevant results are included in Table 6, namely the flexural stress at crack initiation, the flexural strength, toughness index and the average crack spacing.

Table 6

Results of the mechanical tests of composite (coefficient of variation, in %)

Property	REF4F	10RA4F	20RA4F	REF6F	10RA6F	20RA6F
fc (MPa)	18.66	18.91	17.86	18.07	17.17	15.78
	(1.1)	(4.19)	(3.5)	(2.9)	(3.1)	(1.9)
ftd (MPa)	2.23	2.22	2.21	1.95	1.93	1.88
	(1.1)	(3.0)	(1.8)	(0.7)	(9.7)	(3.3)
First cracking strength (MPa)	2.90	3.43	3.06	2.05	2.94	2.33
	(12.4)	(12.8)	(16.0)	(15.5)	(11.3)	(3.6)
Flexural strength (MPa)	3.33	3.53	3.35	2.70	3.78	3.43
	(3.8)	(4.4)	(2.6)	(4.3)	(13.3)	(6.0)
Toughness index I_{20}	20.42	16.94	20.74	20.8	22.22	16.78
	(4.3)	(13.8)	(11,0)	(16.2)	(14.0)	(16.9)
Saturation crack spacing (mm)	25.0	16.7	12.5	4.4	5.9	5.0

3.3.1 Mechanical strength

By analyzing the results of compressive strength, it can be seen that the use of randomly distributed short fibers in cement-based matrices often reduces their compressive strength (Figure 10); the fibers reduce the workability of the material and a greater amount of air is incorporated, making it more porous. In conventional mortar reinforced with relatively low aspect ratio fibers (ARF = 500) a decrease of compressive strength up to about 30% was reported[7]. In the present work, the selfcompacting character of the matrix permitted the incorporation of a higher content of fiber (ARF = 1400) without occurrence of fiber winding or segregation of the mixture. Thus, it was possible to achieve a better fiber distribution and produce a more homogeneous composite.

The indirect tensile strength of composites was not affected by recycled aggregate and neither was it affected by increasing the fiber content. However, the effect of recycled aggregate on flexural behavior indicates an increase of first cracking strength (MPa) and flexural strength (MPa) with an increment of

RA content, compared to reference matrix (with natural aggregate); the maximum increment was about 43% and 40%, respectively.

3.3.2 Flexural behavior of composite

Fig. 9 evidences that the developed composites presented a deflection hardening response with an abrupt decrease of the average crack spacing up to the interval of 5 to 10 mm deflection, followed by a stabilized cracking process up to the end of the tests. As expected, the stabilized cracking process became more premature the higher the fiber content. The flexural behavior begins with an elastic-linear range where the composite material behaves linearly up to a point where the matrix cracks (zone I). The first cracking strength decreases with the increase of the fiber content (up to 29.3%). The post cracking range was characterized by a multiple cracking formation (zone II) until no more cracks are formed. The widening of the existing cracks takes place in region III, where the crack spacing is almost constant, which is similar to that observed by Melo Filho[5]. The flexural stress observed in this region was higher than first cracking strength for all mixtures, indicating the flexural hardening behavior of the developed composites. Due to the relatively low flexural stress at crack initiation in the 20RA6 composite (2.33 MPa), a continuous deflection hardening stage was observed up to the end of the test, at which point an ultimate flexural strength of 3.00 MPa was recorded at a deflection of 27 mm (increase of 47% regarding the flexural stress at crack initiation). In the other composites, a pronounced deflection softening stage was formed with a smooth decrease of the flexural capacity with the evolution of the deflection, caused by the localization and widening of one of the existing cracks (zone IV). Apart from the 20RAF6 composite, this stage initiated at a deflection of around 15 mm.

The crack spacing measurements, as shown in Fig. 9, demonstrate a general reduction in spacing during loading until a steady state condition is reached. This zone covers a large range at the end of Zone II and III and remains constant throughout Zone IV. This constant level of crack spacing, defined as saturation crack spacing (SCS)[35], is presented in Fig. 10 and Table 6. Beyond this point, reduction in crack spacing is not observed, since no new cracks form.
It can be seen that the SCS is inversely proportional to the fiber content for all mixtures. For composite reinforced with Vf=6% the SCS value is up to 5 times lower than composite with 4%. The lowest value obtained for the SCS, 4.4 mm, is comparable to sisal cement composites reinforced with long fibers[5,36].

For composites reinforced with 4% of fiber, a reduction of SCS with increment of recycled aggregate content was reported. This behavior may indicate a higher fiber–matrix bond adhesion for the recycled composite system.

Toughness index values of 16.78 to 22.22 demonstrated the high ductility capacity of the short sisal fiber composite when compared with cement-based matrix. It can be seen that there is no proportionality between the strength (or, toughness) and the fiber content or the recycled aggregate

content separately, indicating that the interaction between these components affects the mechanical behavior of the composite.

3.3.3 Cyclic behavior in bending

In many possible applications of cement-based composites reinforced with sisal fibers, such as the roof or floor of buildings, the presence of dynamic loads is common, which generate loading and unloading cycles on the constructive element. Within the elastic layer, in which the composite is uncracked, limited cyclic loading will have no effect on the performance of the composite. In the post-cracking stage, however, any residual deformations and the subsequent deformational behavior on reloading of the cracked composite become important[37]. In materials subjected to cyclic loading, during the realization of the hysteresis loop, the dissipated energy corresponds to the damping of the material. In composites, the hysteresis loop area can be used as an effective tool for monitoring the progression of the damage under deformation and its damping capacity under usual dynamic loads, such as shock loads or seismic actions.

Fig. 12 shows a schematic representation of the loading-unloading cycles used and experimental typical curve of test. The initial stiffness (Eo) is the stiffness of the uncracked composite obtained by the inclination of the first section of the load-displacement curve. The postcracking stiffness (E1, E2...Ei) was assumed as the inclination of the dashed line connecting points A and B of the hysteresis loop. The degradation of stiffness is the ratio between the stiffness of the cracked composite and the intact composite (Ei / Eo ratio). Evaluating the results shown in Fig. 13, it appears that in the initial stage of cracking, the stiffness degrades rapidly and the dissipated energy increases. According to Holmes and Chu[38], such behavior is associated with multiple cracking of matrix, fiber-matrix debonding and interface wear.

The degradation of stiffness, after the start of cracking, approximately reflects the process of formation of cracks[39] since the matrix (stiffer) reduces its contribution and part of the stress is transferred to the sisal fibers. This degradation occurs throughout the cracking zone II (see Figure 9) and stabilizes in region III when more cracks are not formed, which occurs for deflections of approximately 15 mm. This exponential variation (see Fig. 13) of the stiffness degradation with the crack evolution process is similar to that obtained by Keer[40]. As expected, during the crack formation process, the stiffness degradation was less intense the higher the content of fibers was[41]. The content of fibers had a relatively small influence on the evolution of the stiffness degradation up to the cracking stabilized stage. After this stage, the composites with higher content of fibers presented a larger stiffness degradation than the composites with smaller content of fibers, which can be justified by a more intensive slip between fibers and the surrounding matrix due to the difficulty of assuring proper bond conditions when the content of fiber is appreciable.

The energy dissipated during the unloading-reloading cycles corresponds to the area of the hysteresis loops (hatched area represented inset of Fig. 12a). In this work, the energy dissipated in the

unloading-reloading cycles was normalized by the energy consumed up to 24 mm (area under the envelope of the load versus deflection relationship).

In cracked composite, where the multicracking and fiber/matrix interface debonding are present, the hysteresis loops develop as a result of energy dissipation through frictional slip between fibers and the matrix upon unloading and subsequent reloading[42]. Therefore, the absorbed energy in a load-unload cycle increases as the deformation in which the discharge is applied also increases[40]. However, in Figure 13 a linear increase in the dissipated energy with increment of deflection value of about 13 mm (Vf = 4%) and about 20 mm (Vf = 6%) can be seen. These limits correspond exactly to the end of region II of cracking (described in Section 3.3.2) of the composite, which indicates that the crack opening region (Region III) corresponds, in fact, to a significant reduction in the bond between the short fibers and the cement matrix, with increases of debonding and pullout of the fibers. After this limit, the energy dissipated had a tendency to decrease as a consequence of the softening nature of the structural response of the specimens (smaller load carrying capacity in the post-peak stage).

4. Conclusions

In this paper, the mechanical behavior in early ages of sisal fiber cement composites under flexion is presented. The following conclusions can be drawn based on the results obtained in the present investigation:

1.The use of recycled fine aggregate, despite its large absorption, does not significantly affect the physical and mechanical properties of the mortar and allows for the production of a self-compacting matrix, more appropriate to ensure a homogeneous distribution of the fiber.

2. The sisal fibers, after being subjected to treatment with 10 cycles of wetting and drying, modified their morphology, resulting in reduced fiber lumens, despite the change in the mechanical behaviour under traction.

3. As expected, the addition of short fiber results in a reduction of mechanical strength and elastic modulus but in lesser proportion than that observed in composites with conventional matrices.

4. Under flexion, the process of fracture of all studied composites was characterized by a multiple cracking behavior with deflection hardening. The crack spacing as a function of applied deflection was characterized using an exponential decay function under displacement. The crack saturation spacing in flexure reduces with increase of fiber content and shows, for composites with vf=6%, values similar to that observed in sisal long fiber reinforced cement composites

5. An increase of stress after first cracking and an increase of dissipated energy with cracking of composite can be observed, which characterizes it as a possible sustainable material with structural or semi-structural use. This presents a new perspective for the premise of producing high-performance materials reinforced with natural fiber.

References

1. Roma Jr LC, Martello LS, Savastano Jr H (2008) Evaluation of mechanical, physical and thermal performance of cement-based tiles reinforced with vegetable fibers. *Construction and Building Materials* **22**: 668–674.
2. CEPED (1982) *Utilização de fibras vegetais no fibro-cimento e no concreto-fibra*. BNH-DEPEA, Rio de Janeiro, Brazil.
3. Schafer HG, Brunssen GW (1990) Sisal-Fibre Reinforced Lost Form Work for Floor Slabs. In *Proceedings Second Intl. Symp. of RILEM on Vegetable Plants and their Fibres as Building Materials.* (Sobral, H.S (ed)). London: Chapman and Hall. pp 173-181.
4. Lima PRL (2004) *Análise teórica e experimental de compósitos reforçados com fibras de sisal*. PhD Thesis. PEC/COPPEDEC/UFRJ. Rio de Janeiro, Brazil.
5. Melo Filho JD, Silva FA, Toledo Filho RD (2013) Degradation kinetics and aging mechanisms on sisal fiber cement composite systems. *Cement and Concrete Composites* **40**: 30-39.
6. Norton B and Skates H (2000) Technologies for sustainable buildings. In: *Anals of World Renewable Energy Congress VI* (Edited by Sayigh, A.A.M.). Pergamon, Brighton, UK, part IV, pp 142-147.
7. Lima PRL, Toledo Filho RD, Melo Filho JA (2014) Compressive stress-strain behaviour of cement mortar-composites reinforced with short sisal fibre. *Materials Research* **17(1)**: 38-46.
8. Asprone D, Durante M, Prota A, Manfredi G (2011) Potential of structural pozzolanic matrix–hemp fiber grid composites. *Construction and Building Materials* **25(6)**: 2867-2874.
9. Mohr BJ, Biernacki JJ, Kurtis KE (2007). Supplementary cementitious materials for mitigating degradation of kraft pulp fiber-cement composites. *Cement and Concrete Research* **37(11)**, 1531-1543.
10. Lima PRL and Toledo Filho RD (2008) Uso de metacaulinita para incremento da durabilidade de compósitos à base de cimento reforçados com fibras de sisal. *Ambiente Construído* **8(4)**: 7-19.
11. Corinaldesi V and Moriconi G (2009) Behaviour of cementitious mortars containing different kinds of recycled aggregate. *Construction and Building Materials* **23**: 289-294.
12. Evangelista L and Brito J (2010) Durability Performance of Concrete Made With Fine Recycled Concrete Aggregates. *Cement and Concrete Composites* **32(1)**: 9-14.
13. Lima PRL and Leite MB (2012) Influence of CDW Recycled Aggregate on Drying Shrinkage of Mortar. *Open Journal of Civil Engineering* **2**: 53-57.
14. Chen HJ, Yen T, Chen KH (2003) The use of building rubbles in concrete and mortar. *Journal of the Chinese Institute of Engineers* **26(2)**: 227-236.
15. Gonçalves P, Brito J (2008) Utilização de agregados reciclados em betão. Análise comentada da regulamentação existente. *Engenharia Civil UM* **32**: 73-86.
16. Rong MZ, Zhang MQ, Liu Y, Yang GC, Zeng HM (2001) The effect of fiber treatment on the mechanical properties of unidirectional sisal-reinforced epoxy composites. *Composites Science and Technology* **61**: 1437-1447.

17. Toledo Filho RD, Ghavami K, England GL (2003) Development of vegetable fibre-mortar composites of improved durability. *Cement and Concrete Composites* **25 (2)**: 185-196.

18. Claramunt J, Ardanuy M, Garcia-hortal JA (2010) Effect of drying and rewetting cycles on the structure and physicochemical characteristics of softwood fibres for reinforcement of cementitious composites. *Carbohydrate Polymers* **79**: 200-205.

19. Ferreira SR, Lima PRL, Silva FA, Toledo Filho RD (2014) Effect of Sisal Fiber Hornification on the Fiber-Matrix Bonding Characteristics and Bending Behavior of Cement Based Composites. *Key Engineering Materials (Online)* **600**: 421-432.

20. Ferreira SR (2012) *Influência da hornificação na aderência fibra-matriz e no comportamento mecânico de compósitos cimentícios reforçados com fibras curtas de sisal*, M.Sc. Thesis, UEFS, Feira de Santana, Brasil.

21. Westerholm M, Lagerblad B, Silfwerbrand J, Forssberg E (2008) Influence of fine aggregate characteristics on the rheological properties of mortars. *Cement and Concrete Composites* **30**: 274-282.

22. Lima PRL, Toledo Filho RD, Gomes OFM (2014) Influence of Recycled Aggregate on the Rheological Behavior of Cement Mortar. *Key Engineering Materials* **600**: 297-307.

23. Lima PRL, Santos RJ, Ferreira SR, Toledo Filho RD (2014) Characterization and treatment of sisal fiber residues for cement-based composite application. *Engenharia Agrícola* **34(5)** 812-825.

24. ABNT (ASSOCIAÇÃO BRASILEIRA DE NORMAS TÉCNICAS) (2005) NBR 9778: Argamassa e concreto endurecidos – Determinação da absorção de água, índice de vazios e massa específica. ABNT, Rio de Janeiro.

25. ABNT (ASSOCIAÇÃO BRASILEIRA DE NORMAS TÉCNICAS) (2007) NBR 5739: Concreto – Ensaio de compressão de corpos de prova cilíndricos. ABNT, Rio de Janeiro.

26. ABNT (ASSOCIAÇÃO BRASILEIRA DE NORMAS TÉCNICAS) (1994) NBR 7222: Argamassa e concreto – Determinação da resistência à tração por compressão diametral em corpos de prova cilíndricos. ABNT, Rio de Janeiro.

27. ASTM (American Society for Testing and Materials) (1998) C1018-97: Standard Test Method for Flexural Toughness and First Crack Strength of Fiber-Reinforced Concrete. ASTM, West Conshohocken, PA.

28. Silva FDA, Fairbairn EDMR, Toledo Filho RD, Melo Filho JDA (2010) Physical and mechanical properties of durable sisal fiber–cement composites. *Construction and Building Materials* **24(5)**: 777-785.

29. Diniz JMBF, Gil MH, Castro JAAM (2004) Hornification—its origin and interpretation in wood pulps. *Wood Science Technology* **37**: 489-494.

30. Herrera-Franco PJ and Valadez-Gonzalez AA (2005) A study of the mechanical properties of short natural-fiber reinforced composites. *Composites: Part B* **36**: 597–608.

31. Kim JT, Netravali AN (2010) Mercerization of sisal fibers: effect of tension on mechanical properties of sisal fiber and fiber-reinforced composites. *Composites Part A: Applied Science and Manufacturing* **41(9)**: 1245-1252.

32. Mohan TP and Kanny K (2012) Chemical treatment of sisal fiber using alkali and clay method. *Composites: Part A* **43**: 1989–1998.

33. Fathifalz G, Razaqpur AG, Isgor OB, Abbas A, Fournier B, Foo S (2011) Creep and drying shrinkage characteristics of concrete produced with coarse recycled concrete aggregate *Cement & Concrete Composites* **33**: 1026-1037.

34. Zega CJ and Di Maio AA (2011) Use of recycled fine aggregate in concretes with durable requirements. *Waste Management* **31(11)**: 2336-2340.

35. Katz A (2003) Properties of Concrete Made with Recycled Aggregate from Partially Hydrated Old Concrete. *Cement and Concrete Research* **33(5)**: 703-711.

36. Silva FDA, Mobasher B, Toledo Filho RD (2009) Cracking mechanisms in durable sisal fiber reinforced cement composites. *Cement & Concrete Composites* **31**: 721–730

37. Keer JG (1981) Behaviour of cracked fibre composites under limited cyclic loading. *International Journal of Cement Composites and Lightweight Concrete* **3(3)**: 179-86.

38. Holmes JW, Cho C (1992). Experimental Observations of Frictional Heating in Fiber- Reinforced Ceramics. *Journal of the American Ceramic Society* **75(4)**: 929-938.

39. Jun P and Mechtcherine V (2010) Behaviour of Strain-hardening Cement-based Composites (SHCC) under monotonic and cyclic tensile loading. *Cement & Concrete Composites* **32**: 810–818.

40 Keer JG (1985) Some observations on hysteresis effects in fibre cement composites. *Journal of materials science letters* **4**: 363-366.

41. Barros JAO, Cruz JMS, Delgado RM, Costa AG (2000) Reinforced concrete under cyclic loading. In *Proceedings of the 12th World Conference on Earthquake Engineering*. vol. 9. no. 0772. New Zealand, pp.1–8.

42 Longbiao L (2015) A hysteresis dissipated energy-based damage parameter for life prediction of carbon fiber-reinforced ceramic-matrix composites under fatigue loading. *Composites Part B* **82**: 108-128.
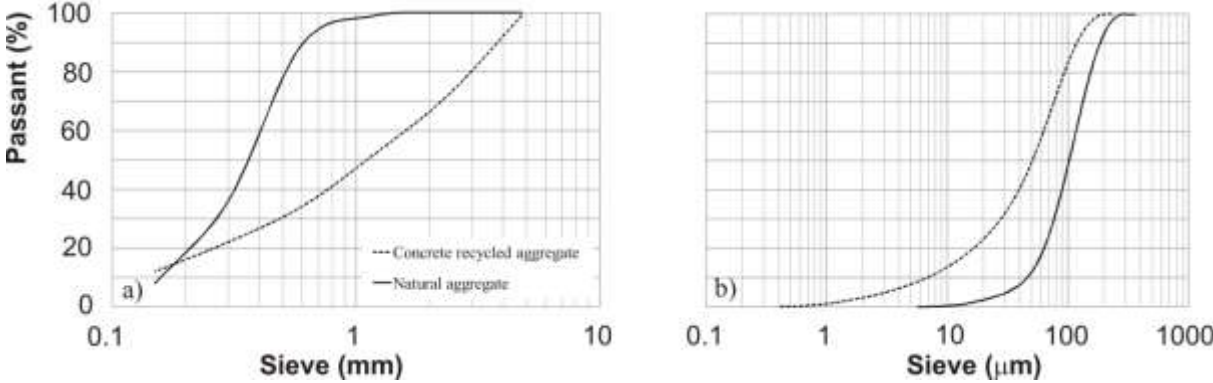
Figure captions

Figure 1. Granulometric analysis: a) grading curves of the aggregates; b) size distribution of particles passing in 150 μm.
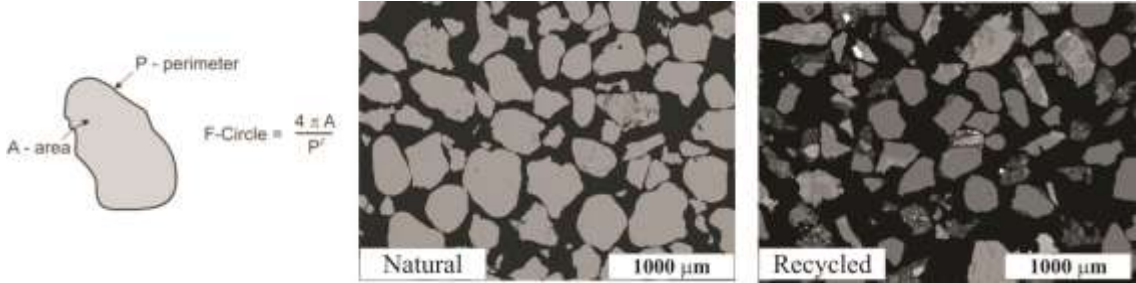
Figure 2. Determination of the circular shape factor (F-circle) of natural and recycled sands particles
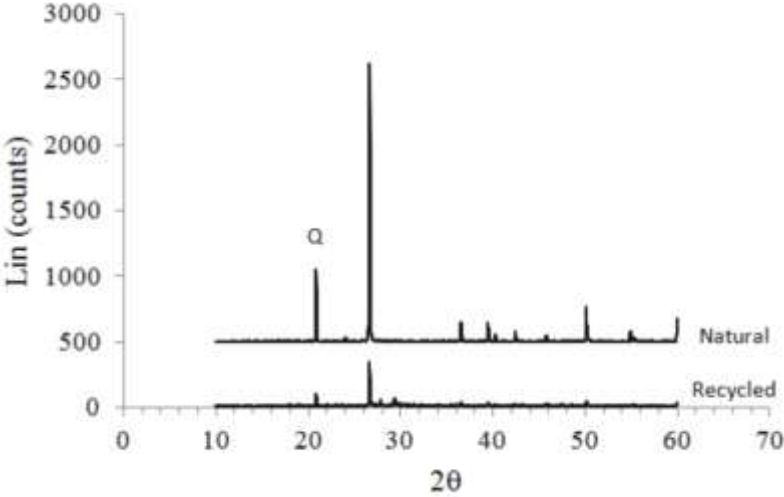
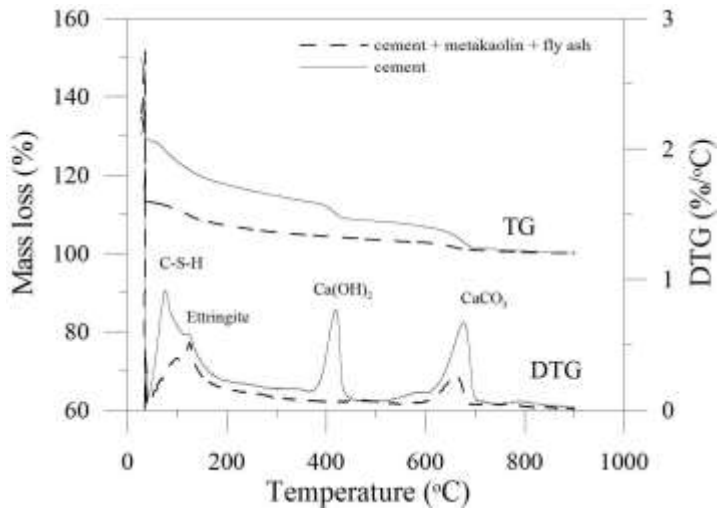Figure 3. X-ray diffraction pattern of aggregates

Figure 4. TG and DTG curves of the cement pastes with and without additions
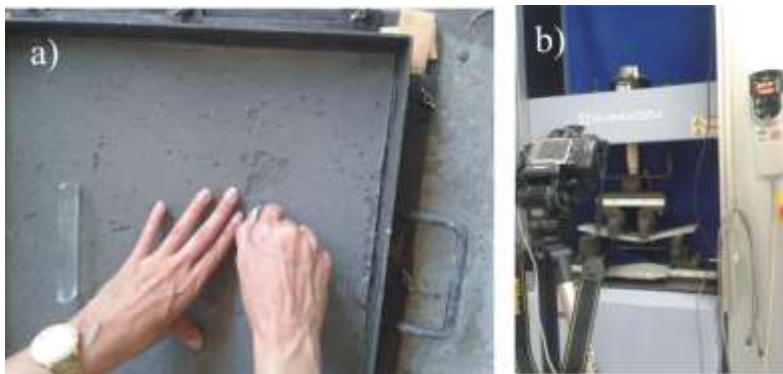
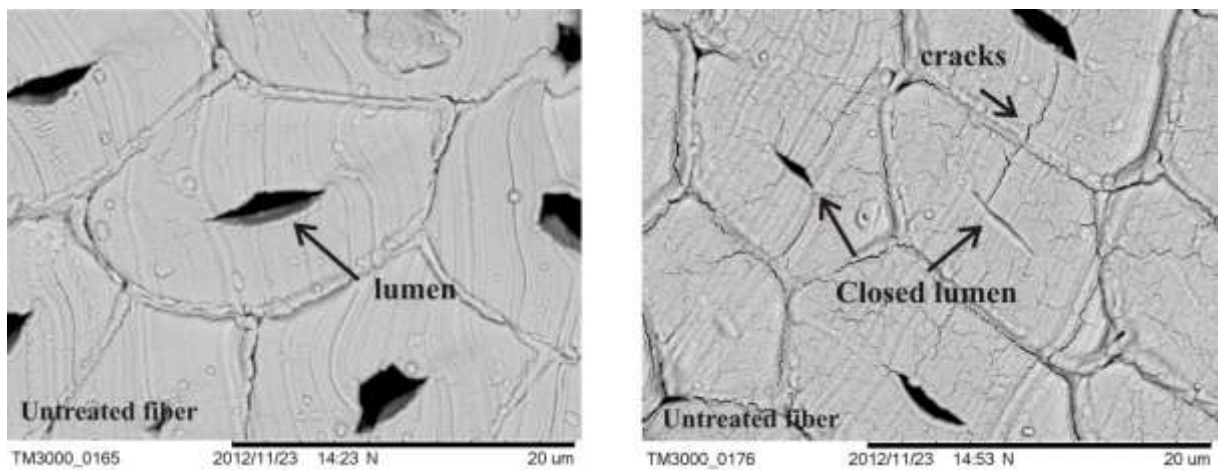Figure 5. Flexural test: a) Production of the composite; b) test setup

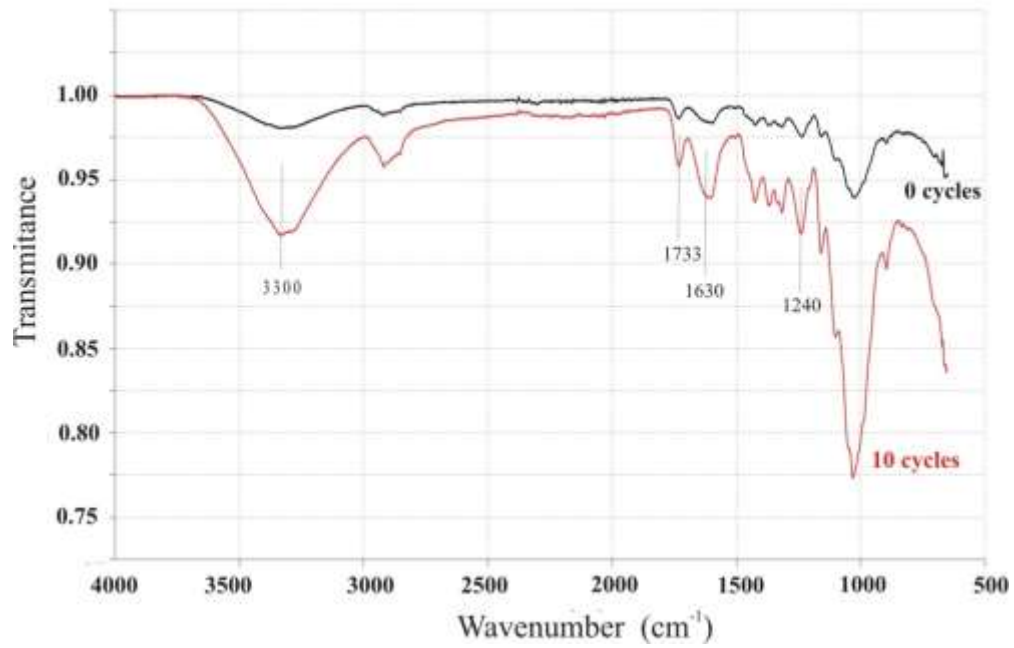Figure 6. Effect of treatment on sisal fiber morphology

Figure 7. Fourier transform infrared (FTIR) spectrum for treated (10 cycles) and untreated sisal fiber
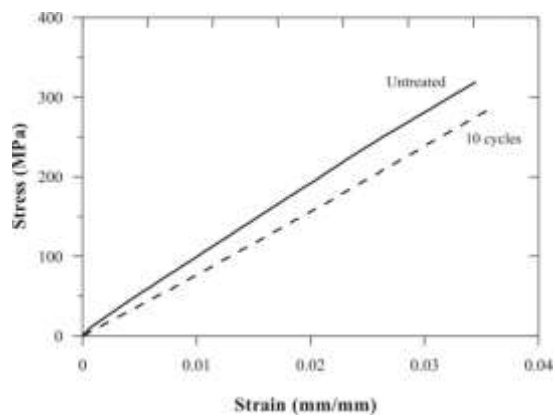
Figure 8. Effect of treatment on stress-strain behavior of fiber

Figure 9. Flexural stress versus central deflection relationship and average crack spacing evolution for the composites

Figure 10. Influence of type of matrix and fiber aspect ratio on the compressive strength of sisal-cement composites

Figure 11. Effect of fiber volume on cracking pattern

Figure 12. Flexural cyclic tests: a) Determination of properties; b) Typical experimental load versus deflection relationship (Vf = 6%)

Figure 13. Relationship between deflection and both the normalized dissipated energy and stiffness degradation

Figures

Figure 1. Granulometric analysis of the aggregates: a) grading curves; b) size distribution of particles passing in 150 μm.

Figure 2. Determination of the circular shape factor (F-circle) of natural and recycled sands particles

Figure 3. X-ray diffraction pattern of aggregates

Figure 4. TG and DTG curves of the cement pastes with and without additions

Figure 5. Flexural test: a) Production of the composite; b) test setup

Figure 6. Effect of treatment on sisal fiber morphology

Figure 7. Fourier transform infrared (FTIR) spectrum for treated (10 cycles) and untreated sisal fiber

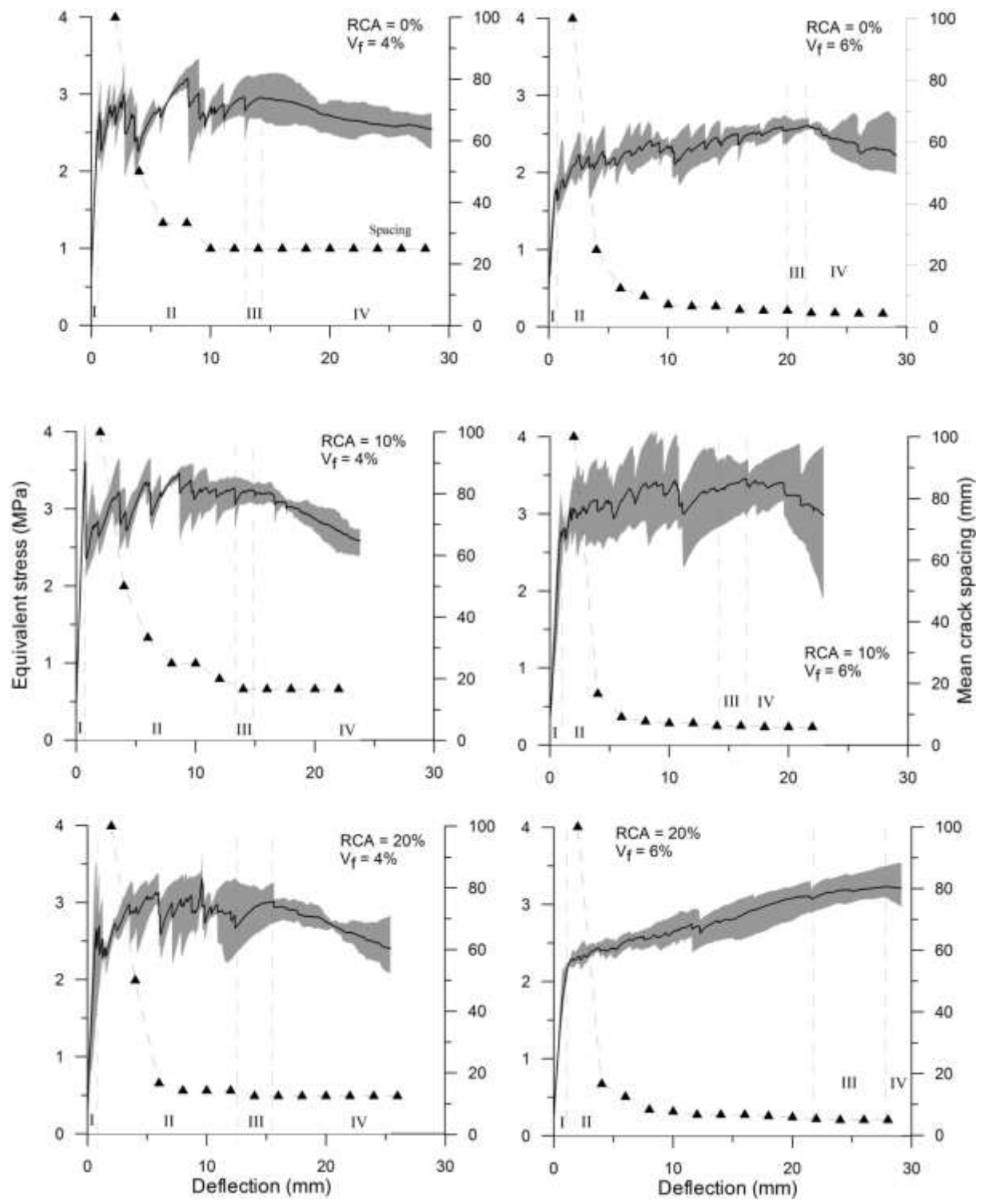Figure 8. Effect of treatment on stress-strain behavior of fiber

Figure 9. Flexural stress versus central deflection relationship and average crack spacing evolution for the composites
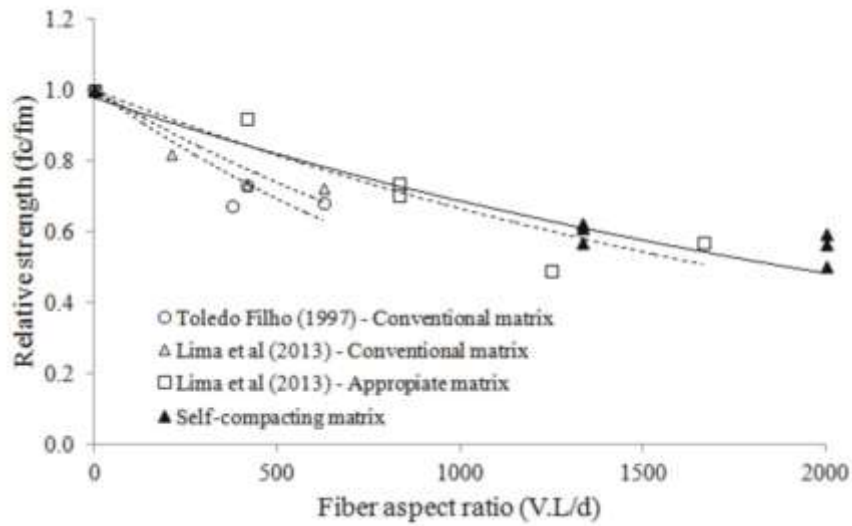
Figure 10. Influence of type of matrix and fiber aspect ratio on the compressive strength of sisal-cement composites

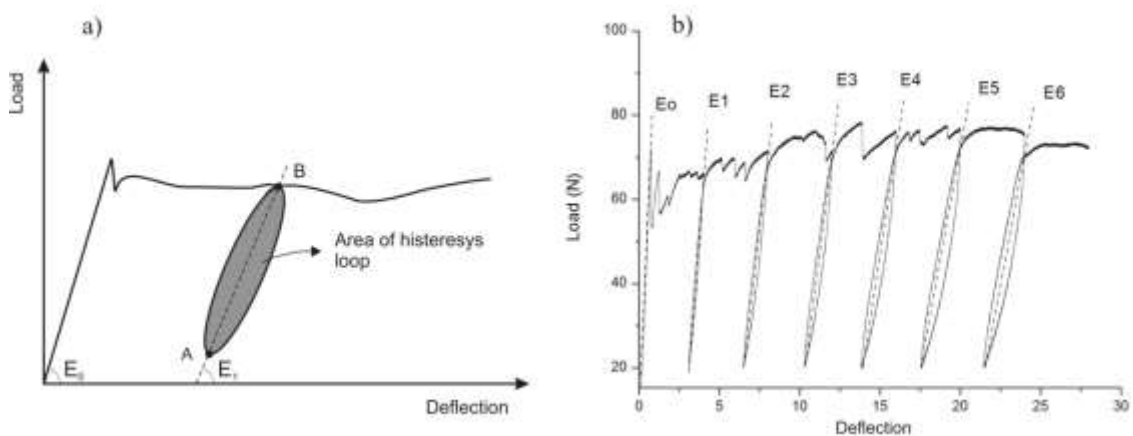

Figure 11. Effect of fiber volume on cracking pattern

Figure 12. Flexural cyclic tests: a) Determination of properties; b) Typical experimental load versus deflection relationship (Vf = 6%)
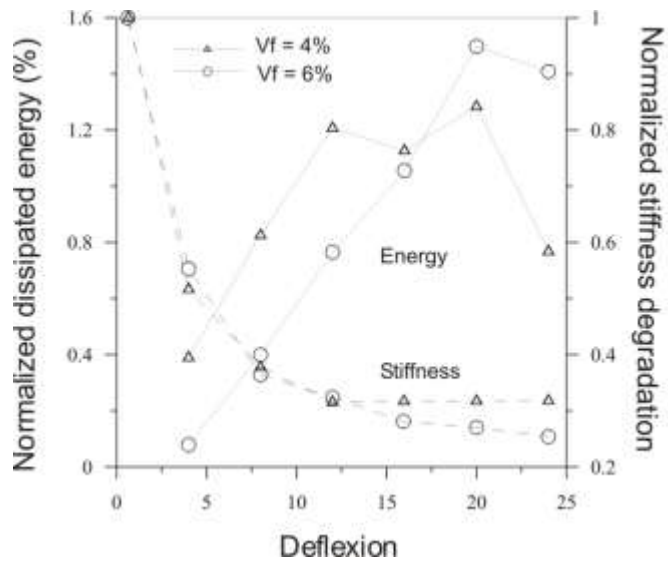
Figure 13. Relationship between deflection and both the normalized dissipated energy and stiffness degradation